AIP Journal of Applied Physics

Dielectric properties of (110) oriented Pb Zr O 3 and La-modified Pb Zr O 3 thin films grown by sol-gel process on Pt (111) ⁄ Ti ⁄ Si O 2 ⁄ Si substrate

Jayanta Parui and S. B. Krupanidhi

Citation: Journal of Applied Physics **100**, 044102 (2006); doi: 10.1063/1.2234819
View online: http://dx.doi.org/10.1063/1.2234819
View Table of Contents: http://scitation.aip.org/content/aip/journal/jap/100/4?ver=pdfcov
Published by the AIP Publishing

Articles you may be interested in
Energy-storage performance and electrocaloric effect in (100)-oriented Pb0.97La0.02(Zr0.95Ti0.05)O3 antiferroelectric thick films
J. Appl. Phys. **110**, 064109 (2011); 10.1063/1.3641983

Dielectric relaxation of Sr1–1.5 x Bi x TiO3 sol-gel thin films
J. Appl. Phys. **109**, 064103 (2011); 10.1063/1.3549612

Deposition of sol-gel derived lead lanthanum zirconate titanate thin films on copper substrates
Appl. Phys. Lett. **92**, 252905 (2008); 10.1063/1.2945887

Characterization of (100)-oriented Bi Sc O 3 – Pb Ti O 3 thin films synthesized by a modified sol-gel method
Appl. Phys. Lett. **88**, 222904 (2006); 10.1063/1.2208961

Dielectric properties of oriented PbZrO 3 thin films grown by sol-gel process
J. Appl. Phys. **92**, 3990 (2002); 10.1063/1.1505981

[This article is copyrighted as indicated in the article. Reuse of AIP content is subject to the terms at: http://scitation.aip.org/termsconditions. Downloaded to] IP: 128.189.204.254 On: Thu, 11 Dec 2014 11:37:02

Dielectric properties of (110) oriented $PbZrO_3$ and La-modified $PbZrO_3$ thin films grown by sol-gel process on Pt(111)/Ti/SiO_2/Si substrate

Jayanta Parui and S. B. Krupanidhi[a)]
Materials Research Center, Indian Institute of Science, Bangalore 560012, India

(Received 13 November 2005; accepted 6 June 2006; published online 17 August 2006)

Highly (110) preferred orientated antiferroelectric $PbZrO_3$ (PZ) and La-modified PZ thin films have been fabricated on Pt/Ti/SiO_2/Si substrates using sol-gel process. Dielectric properties, electric field induced ferroelectric polarization, and the temperature dependence of the dielectric response have been explored as a function of composition. The T_c has been observed to decrease by ~ 17 °C per 1 mol % of La doping. Double hysteresis loops were seen with zero remnant polarization and with coercive fields in between 176 and 193 kV/cm at 80 °C for antiferroelectric to ferroelectric phase transformation. These slim loops have been explained by the high orientation of the films along the polar direction of the antiparallel dipoles of a tetragonal primitive cell and by the strong electrostatic interaction between La ions and oxygen ions in an ABO_3 perovskite unit cell. High quality films exhibited very low loss factor less than 0.015 at room temperature and pure PZ; 1 and 2 mol % La doped PZs have shown the room temperature dielectric constant of 135, 219, and 142 at the frequency of 10 kHz. The passive layer effects in these films have been explained by Curie constants and Curie temperatures. The ac conductivity and the corresponding Arrhenius plots have been shown and explained in terms of doping effect and electrode resistance. © *2006 American Institute of Physics*. [DOI: 10.1063/1.2234819]

I. INTRODUCTION

Antiferroelectric-type thin films have been extensively investigated for potential applications in integrated devices.[1] In recent years, they have been recognized as the potential candidates for sensor and actuator applications in microelectromechanical systems (MEMSs) through the combination with silicon micromachining technology with which the actuator devices, including micropositioners, micromotors, microvalves, and micropumps, can be widely used in compact medical, automative, optical, and space systems.[2,3] Electric field induced strains in ferroelectric and antiferroelectric materials can occur by three mechanisms such as piezoelectricity, electrostriction, and phase switching. While the piezoelectric effect in lead zirconate titanate (PZT) thin films is still under investigation for microactuator application, it is necessary to develop other materials that can generate higher strain levels.[4,5] Antiferroelectric (AFE) to ferroelectric (FE) phase switching materials may be one of the alternatives, which has the potential to work in thin film form. Electrostrictive materials represented by relaxor ferroelectrics, which include La-modified PZT (PLZT) and lead magnesium niobate (PMN), exhibit large nonlinear electromechanical behavior with minimum hysteresis.[6] For induced phase transformation materials, e.g., PZ and Sn-modified PZT (PZST), a strain develops under bias due to a field-forced AFE-FE phase transformation. The latter has been suggested for the use in large strain, high force actuators[7–9] due to a large transformational strain of ~1%.

However, it has been reported that for bulk PZ ceramics AFE-FE phase transformations were observed only near a Curie point (~230 °C).[10] From the crystallographic viewpoint, the AFE phase has an orthorhombic structure where an orthorhombic cell is a multiple unit cell and contains eight primitive cells, which have a tetragonal structure.[11] The polar direction of the antipolar dipoles is along the (110) direction of the tetragonal primitive cell.[12] When changed to the FE phase, the tetragonal primitive cell becomes rhombohedral with the polar directions along the (111) direction.[13] However, the field-forced AFE-FE structural transformation of highly (110) oriented PZ thin films have not been investigated in detail, especially with *A*-site donor doping for minimum hysteresis loss, and in our present investigation, we have chosen La for its strong electrostatic interaction with oxygen ions in an ABO_3 perovskite unit cell.

In 1985, the preparation of PZ thin layers was reported by Budd *et al.*[14] and in 1992, Wang *et al.*[15] reported the preparation of acetate precursor derived layers. In general, PZ layers were reported as more susceptible to cracking and resistant to crystallization than lead titanate (PT) or PZT layers. In addition to that, Tani *et al.* reported the preparation of highly (111) and (100) oriented PZ thin films by precursor route.[16] It is worthy to inform that there are several other routes that have been applied for the preparation of PZ thin films, which include the epitaxial PZ films on $SrTiO_3$ substrates by metal-organic chemical vapor deposition[17] (CVD) and *c*-axis-oriented PZ layer on Si substrates by pulsed laser deposition (PLD).[18] Though La-modified PZ thin films were reported by Bharadwaja and Krupanidhi,[19] the minimum doping level was 3 mol %, whereas Dai *et al.*[20] reported minimum doping level of 1 mol%, in the case of bulk materials. In this paper, we have described the sol-gel preparation

[a)]Author to whom correspondence should be addressed; electronic mail: sbk@mrc.iisc.ernet.in

[This article is copyrighted as indicated in the article. Reuse of AIP content is subject to the terms at: http://scitation.aip.org/termsconditions. Downloaded to] IP: 128.189.204.254 On: Thu, 11 Dec 2014 11:37:02

of PZ and La-modified PZ thin layers with preferred orientation and subsequent characterization of properties. The electric field and temperature-induced phase transformation behavior are discussed.

II. EXPERIMENTAL PROCEDURES

A. Thin layer preparation

The preparation method used to fabricate PZ and La-modified PZ thin layers was quite similar to that used recently for PZT thick films.[21] The solutions were prepared from starting solutions of molar compositions of $Pb(CH_3COO)_2 \cdot 3H_2O$:zirconium *n*-butoxide:polyvinylpyrrolidone(PVP):acetyl acetone:2-methoxyethanol $=1.1:1:0.7:0.5:30$, where the mole ratio for PVP is defined for the monomer (the polymerizing unit). First, $Pb(CH_3COO)_2 \cdot 3H_2O$ was dissolved in 2-methoxyethanol and then zirconium *n*-butoxide was added to the solution followed by acetyl acetone. The resultant solution was refluxed at 70 °C for 2 h. followed by cooling down to room temperature. A prescribed amount of PVP (40 000 in average molecular weight) was added and dissolved by stirring. The solution was diluted by the addition of 2-methoxyethanol to adjust the solution molarity to 0.3*M*. Then the solution was deposited on $Pt(111)/Ti/SiO_2/Si$ substrates by spin casting at 3500 rpm for 30 s. After each coating the film was pyrolyzed at 350 °C for 5 min. Then after six coatings the film was annealed at 750 °C for 30 min in an oxygen-rich environment. In the case of La doping $Pb(CH_3COO)_2 \cdot 3H_2O$ and $La(NO_3)_3 \cdot 6H_2O$ together dissolved in 2-methoxyethanol. Thickness of the crystalline films was observed to be varied from ~0.6 to ~0.8 μm. The crystallization behavior was examined after heat treatment by x-ray diffraction (XRD) (Scintag 3100) and surface morphology, and film thickness was determined by scanning electron microscopy (SEM).

B. Electrical property measurements

Circular gold electrodes of around 1.693×10^{-3} cm^2 were deposited onto the top surface of the films by means of shadow masking. A portion of the films was then etched away with hydrofluoric acid and the Pt layer exposed for a bottom electrode. Weak-field dielectric measurements were determined on an impedance analyzer (Keithley 3330 *LCZ* meter) using a driving voltage of 200 mV measured at $40-10^5$ Hz. High-field hysteresis measurements were made on Sawyer-Tower circuit (RT-66A) and high-field capacitance versuss. voltage measurements were made using impedance analyzer and voltage source (Keithley 230 Programmable Voltage Source) at 1, 10, and 100 kHz. Temperature dependent measurements were made in closed box where films were kept on a proportional-integral-differential (PID) controlled heater slab.

III. RESULTS AND DISCUSSION

A. Characterization

XRD patterns taken at room temperature from the films after crystallization at 750 °C for 30 min are shown in Fig. 1. The figure depicts three different XRD patterns where a stands for pure PZ and b and c represent 1 and 2 mol % La-modified PZ thin films, respectively. In every case, it is clearly seen that the films have preferred pseudocubic (110) orientation. The preferred orientation of PZ films can be explained by the formation of Pt_3Pb at the interface of PZ and $Pt/Ti/SiO_2/Si$.[22–25] Though the formation of (111) oriented Pt_3Pb was mentioned by Chen and Chen[22] and Huang *et al.*,[24] it is clear from their studies that the appearance of a particular orientation is not only temperature dependent but also time dependent. So formation of (110) oriented Pt_3Pb within the course of our deposition would be the most possible reason to seed (110) oriented PZ films because the lattice constant of Pt_3Pb $a=4.05$ Å and the lattice constants of the tetragonal phase of PZ are $a=4.16$ Å and $c=4.10$ Å (JCPDS card No.[51] 3-655), which indicate a lattice mismatch of 2.7%. Hence, the above-mentioned reason is suspected as the enhancing factor for the growth of (110) preferred oriented PZ films.

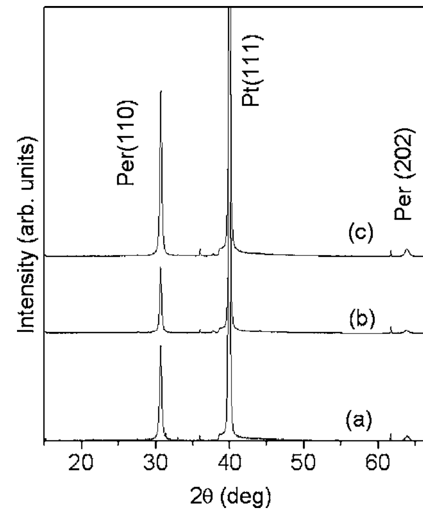

FIG. 1. XRD pattern of (a) pure PZ, (b) 1 mol % La doped PZ, and (c) 2 mol % La doped PZ thin films. Each film was deposited on $Pt(111)/Ti/SiO_2/Si$ substrates and annealed at 750 °C for 30 min.

Figure 2 shows the cross sectional and surface SEM micrographs of three films. From the cross sectional SEM micrograph, the film thicknesses were estimated. The pure PZ thin film has the thickness of 0.68 μm whereas 1 and 2 mol %, La-modified PZ thin films have the thicknesses of 0.8 and 0.62 μm, respectively. However, the surface micrograph shows that pure PZ films are porous in nature, and it has been observed that with La modification the porosity has decreased. In case of (111) preferred oriented PZT thin films, it has been reported that film porosity decreases on La doping along with grain size.[26] In the case of (110) preferred oriented PZ, whether it is the effect of La doping or the effect of surface reconstruction during the extended annealing period is currently under investigation. The cross sectional SEM images are, however, seen to be of dense feature and indicate an active role of the solution ingredients.

B. Polarization Hysteresis

Figure 3 illustrates the *P-E* hysteresis loop, ε-*V*, and tan δ-*V* measurements at 80 °C for PZ and La-modified PZ,

[This article is copyrighted as indicated in the article. Reuse of AIP content is subject to the terms at: http://scitation.aip.org/termsconditions. Downloaded to] IP: 128.189.204.254 On: Thu, 11 Dec 2014 11:37:02

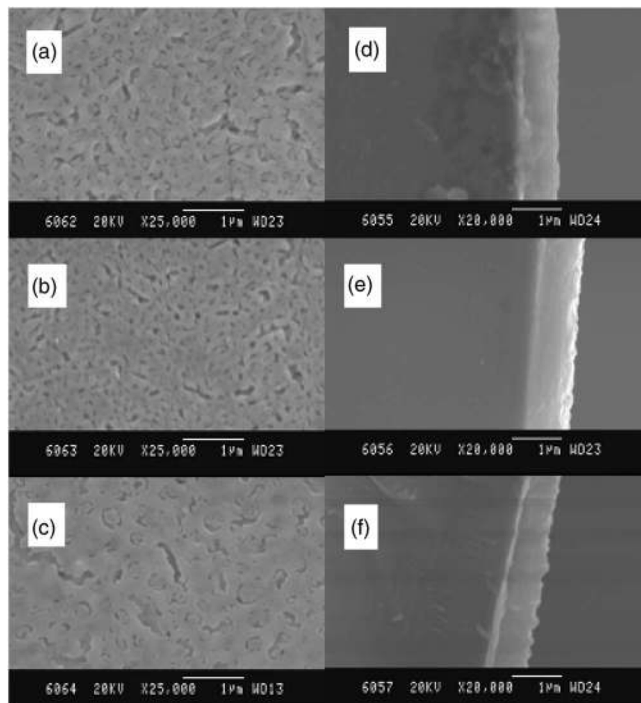

FIG. 2. SEM micrographs of surfaces and cross sections of [(a) and (d)] pure PZ, [(b) and (e)] 1 mol % La doped PZ, and [(c) and (f)] 2 mol % La doped PZ thin films. The thicknesses of pure PZ, 1 mol % La doped PZ, and 2 mol % PZ thin films are 0.68, 0.8, and 0.62 μm, respectively.

which have the preferred (110) orientation in a pseudocubic system. No saturation has been observed in the polarization hysteresis, which may be due to residual stress. However, their tendency towards the ferroelectric loops from antiferroelectricity is the proof of the existence of AFE-FE field-forced phase transformation in those films. It is reported that coercive field for pure PZ is $\sim$250 kV/cm,[15] whereas present films are measured applying maximum $\sim$270 kV/cm electric field at 80 °C, which have exhibited relatively clear double hysteresis loops. It has been seen that for pure PZ, AFE-FE transition field is 176 kV/cm and FE-AFE transition field is 125 kV/cm with reasonably zero remnant polarization, whereas for 1 mol % La doped PZ and 2 mol% La doped PZ, those are 176 and 125 kV/cm, and 193 and 161 kV/cm, respectively. This observation can be explained by coupling between the sublattices of the AFE phase that becomes weaker with the increase of temperature indicating the decrease in coercive field in AFE-FE phase transformation.[9] It is reported that the polar direction of the antipolar dipoles are along the (110) direction of the tetragonal primitive cell,[12] and on the application of electric field, the transition from antipolar to polar dipole ordering is followed by a large jump of the unit cell volume $\Delta V = 0.35$ Å^3 with the change of unit cell parameters.[27] According to Shirane and Hoshino[13] in the rhombohedral structure, the ferroelectricity may be due to parallel displacement of Zr or Pb ions along a (111) direction and the associated displacements of three oxygen ions, whereas under a strong electric field, the antiparallel dipole arrangement in the (110) direction is forced to change to the parallel one. So, when the field-assisted phase transformation leads to a rhombohedral phase, which has an α value just less than 90°,[13,27] it exhibits polarization along the (111) direction. In our case, the electric field direction was identified along the normal to the film, which should be the (110) plane normal of the rhombohedral PZ because of its α value. So the polarization response, after field induced phase transformation, will be small as it is just a component along the (110) direction. Thus, due to high orientation along (110), polarization versus applied electric field hysteresis response of the films was observed to be slimmer. According to von Hippel,[28] if a dopant ion on the A site of an ABO_3 perovskite has stronger interaction with oxygen, the bond between B–O restrains more and disturbs more of the BO_6 network. In the present case, A-site dopant ion La has stronger interaction with oxygen restraining Zr–O bonds. In Fig. 2, it is clearly shown that on application of electric field the ferroelectric loops have become slim on La modification as usually seen in the case of A-site La doping in PZT.[29,30] In Fig. 2 it is clearly represented that ε-V and tan δ-V measurements support the nature of P-E hysteresis loops along with the explanation given above.

C. Dielectric properties

Figure 4(a) shows the dielectric constants (ε) and loss factors (tan δ) for (110) preferred oriented PZ and La-modified PZ thin films as a function of temperature (T) between 26 and 300 °C. The room temperature dielectric constant for pure PZ films is 135 with 0.86% loss factor at a frequency of 10 kHz, whereas 1 mol % La doped and 2 mol. % La doped films have the dielectric constants of 219 and 145 and loss factors of 1.45% and 0.51%, respectively at the same frequency. It was reported by Bharadwaja and Krupanidhi[19] that with the increase of La doping, the room temperature dielectric constant of PZ thin films increases. The present study shows the increase in dielectric constant for 1 mol % La doping, whereas subsequent extent of doping reduced the dielectric constant. The thickness dependence in room temperature dielectric constants of thin films is mainly affected by film-electrode interfaces. These interfaces are generally of low-ε paraelectric in nature due to stoichiometric deviation from bulk grains. Hence, the total capacitance is considered equivalent to the series combination of interface and bulk antiferroelectric capacitors. These interferences show increased dielectric constant with increasing thickness in submicron scale.[31] Thus it is difficult to explain the decrease in dielectric constant in 2 mol % La doped PZ film and increase in dielectric constant in 1 mol % La doped PZ. But according to Bharadwaja and Krupanidhi,[31] at thicknesses $\sim$0.6 μm and above, film-electrode interface effect was shown to be nominal on dielectric property. Hence the dielectric properties shown in Fig. 4 are believed to be the doping effect of La. However, in Fig. 4(b) it is shown that the dielectric response of pure PZ having a maximum value near 230 °C on heating and 225 °C on cooling and the observation are justified as reported in the case of bulk PZ crystals.[10] In the case of 1 and 2 mol % doped thin films, they have the maximum values near 215 and 194 °C on heating and 210 and 189 °C on cooling. Decrease in transition temperature (T_{max}) has been observed depending on the

[This article is copyrighted as indicated in the article. Reuse of AIP content is subject to the terms at: http://scitation.aip.org/termsconditions. Downloaded to] IP: 128.189.204.254 On: Thu, 11 Dec 2014 11:37:02

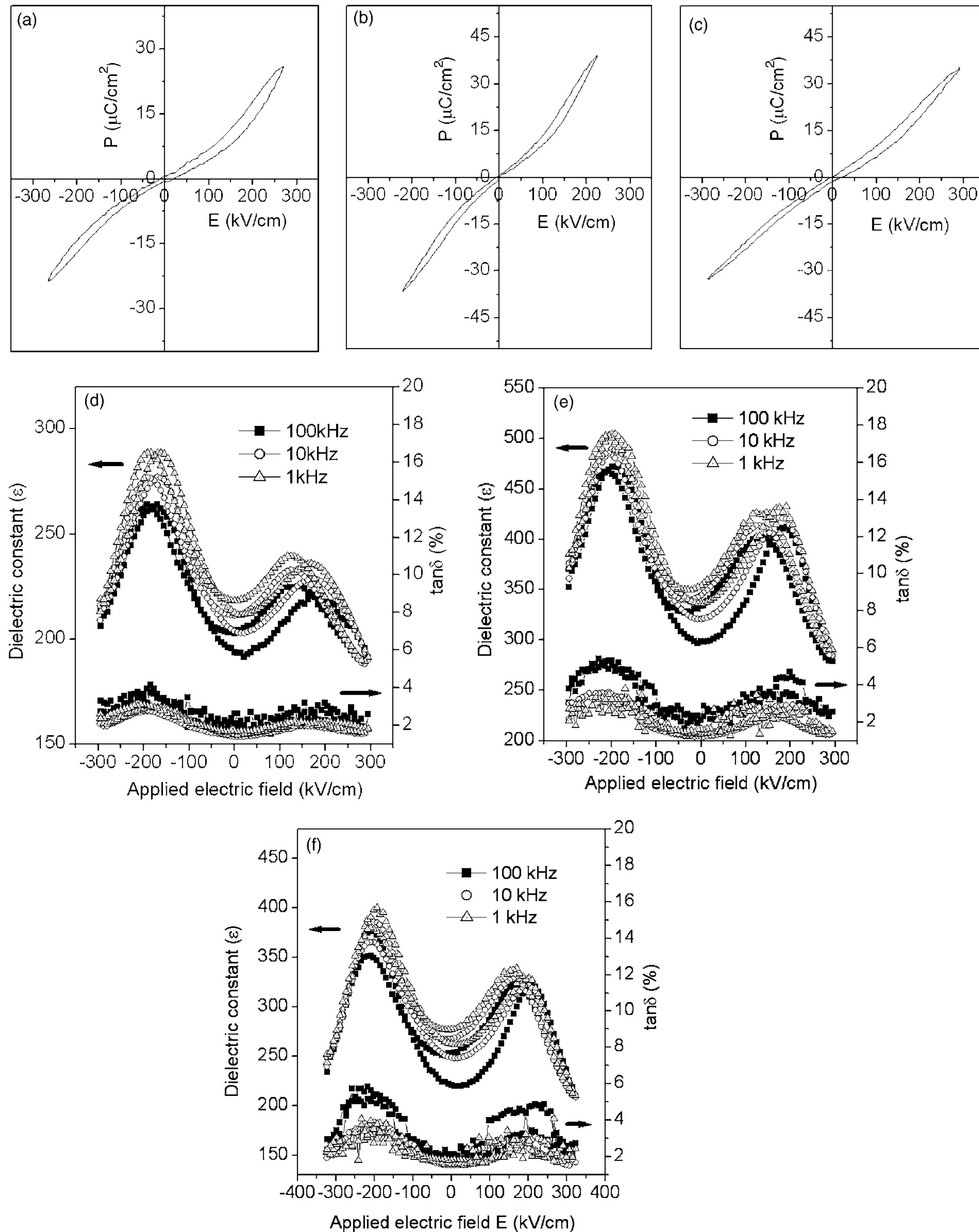

FIG. 3. *P-E* hysteresis behavior of (a) pure PZ, (b) 1 mol % La doped PZ, and (c) 2 mol % La doped PZ thin films and ε-*E* and tan δ-*E* behaviors of (d) pure PZ, (e) 1 mol % La doped PZ, and (f) 2 mol % La doped PZ thin films measured at 80 °C.

extent of La doping, and this may be associated with the strong interaction between La–O, giving rise to an easily switchable polarization state of ZrO_6 network. Under this condition, relatively small thermal energy is sufficient for phase transition. In our present case, relaxor type of behavior on La doping can be justified with its spreadout nature in dielectric constant peak at T_{max}.[32] In Fig. 4(a), we have represented the effect of La modification on phase transition of PZ thin films at frequency of 10 kHz. In addition, in Figs. 4(b)–4(d) we have shown ε vs T and tan δ vs T studies for individual films at 1, 10, and 100 kHz.

D. Effect of passive layer

It is well known that the dielectric property of a thin film is affected by its structural heterogeneity.[33–37] This heteroge-

[This article is copyrighted as indicated in the article. Reuse of AIP content is subject to the terms at: http://scitation.aip.org/termsconditions. Downloaded to] IP: 128.189.204.254 On: Thu, 11 Dec 2014 11:37:02

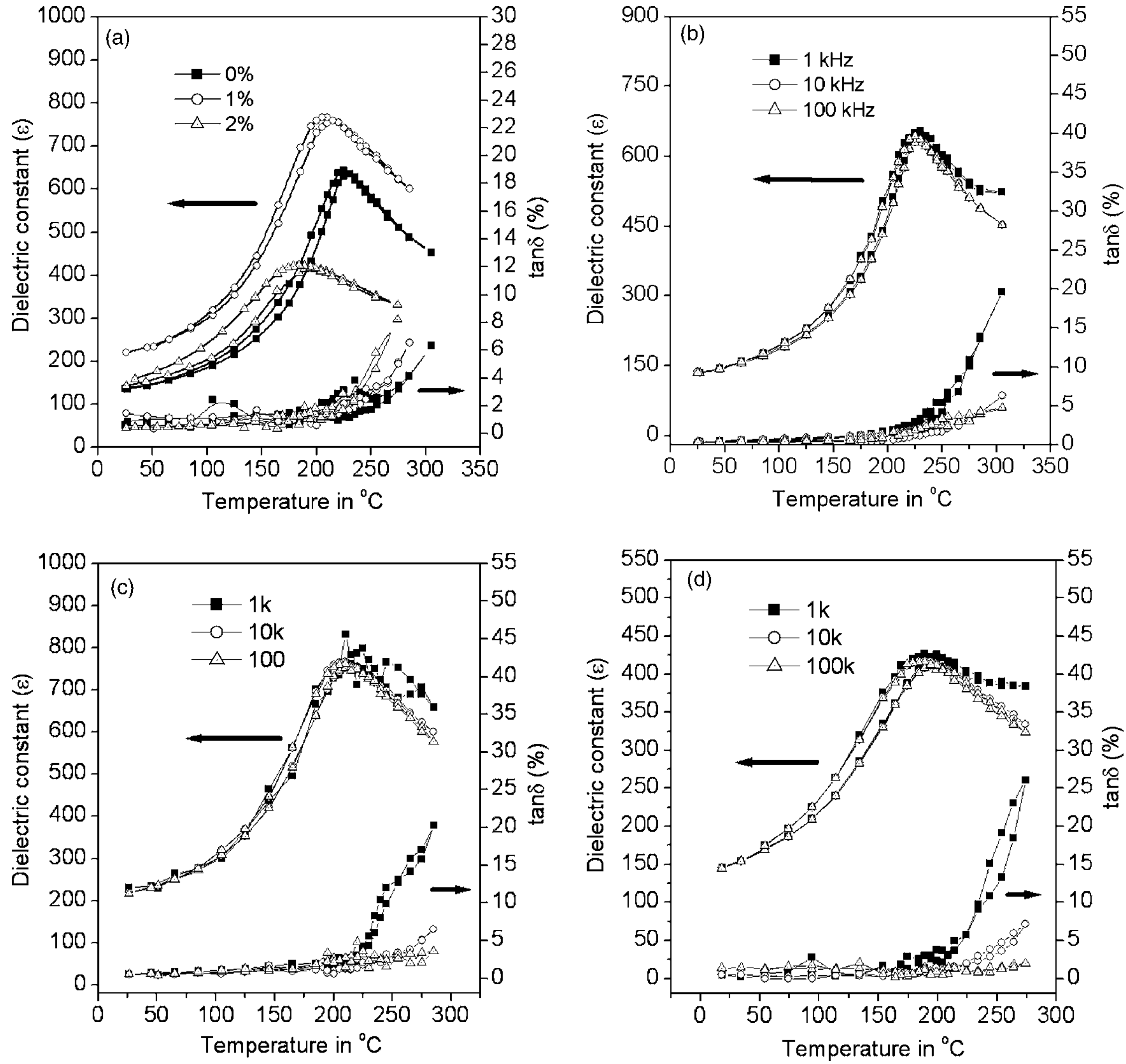

FIG. 4. Temperature-dependent dielectric constant and loss for (a) pure PZ and La-modified PZ measured at 10 kHz, whereas (b), (c), and (d) represent same measurements at different frequencies for pure PZ, 1 mol % La doped PZ, and 2 mol % La doped PZ thin films, respectively.

neity has been modeled, assuming a stacked capacitor structure. The capacitance of the heterostructured film, C_h, is then determined by the capacitance of the pure film, C_f, and the capacitance of the passive layer, C_i, connected in series:

$$\frac{1}{C_h} = \frac{1}{C_f} + \frac{1}{C_i}. \tag{1}$$

Assuming that the thickness of the interface passive layer, d_i, is much smaller than the thickness of the film, d_f, i.e., $d_i \ll d_f$, the dielectric permittivity of the heterostructured film, ε_h, can be evaluated:

$$\frac{1}{\varepsilon_h} = \frac{1}{\varepsilon_f} + \frac{d_i}{d_f \varepsilon_i}. \tag{2}$$

As we know that above Curie temperature θ, the dielectric permitivity of the paraelectric phase of ferroelectrics or antiferroelectrics obeys the Curie-Weiss law,[38]

$$\varepsilon = \frac{c}{T - \theta}, \tag{3}$$

where c is the Curie constant. If the films obey Eq. (3), from the Eqs. (2) and (3) we can write

$$\frac{1}{c_h}(T - \theta_h) = \frac{1}{c_f}(T - \theta_f) + \frac{d_i}{d_f \varepsilon_i}, \tag{4}$$

where the indices h and f refer to the heterostructure and the film, respectively. According to Tyunina and Levoska,[38] if we assume that the capacitance of the passive layer is temperature independent, we get

$$c_h = c_f = c, \tag{5}$$

$$\theta_h = \theta_f - c\frac{d_i}{d_f \varepsilon_i}. \tag{6}$$

On the other hand, if passive layer capacitance is temperature dependent and if we take first approximation, i.e.,

[This article is copyrighted as indicated in the article. Reuse of AIP content is subject to the terms at: http://scitation.aip.org/termsconditions. Downloaded to] IP: 128.189.204.254 On: Thu, 11 Dec 2014 11:37:02

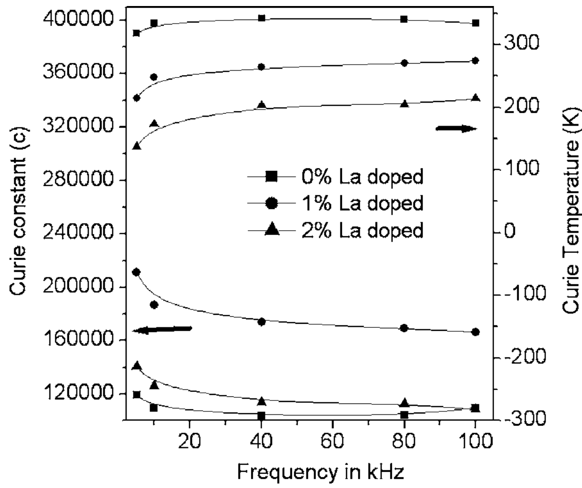

FIG. 5. Frequency dispersion of Curie constants and Curie temperatures for pure and doped PZ thin films according to the Curie-Weiss law.

$$\frac{d_i}{d_f \varepsilon_i} = \frac{1}{c_i} T, \tag{7}$$

the relations become

$$\frac{1}{c_h} = \frac{1}{c_f} + \frac{1}{c_i}, \tag{8}$$

$$\theta_h = \theta_f \left(1 + \frac{c_f}{c_i} \right)^{-1}. \tag{9}$$

In our films, Curie constants and Curie temperatures are calculated at different frequencies. It is shown in Fig. 5 that Curie constants decrease with increase in frequency in the case of doped PZ films, and in the case of pure PZ film, it has been observed to decrease at lower frequency region and seen to increase at higher frequency region. A totally opposite phenomenon has been noticed in the case of Curie temperatures. It has been clearly seen that Curie temperatures increase with the increase in frequency in the case of doped PZ films, whereas in pure PZ film it has been seen to increase at lower frequency region and to decrease at higher frequency region. According to Eqs. (8) and (9), such frequency dispersion in Curie temperature value indicates the frequency dependence of the passive layer. But according to Eq. (8) if the thickness of the passive layer is temperature dependent, there should be a frequency dispersion in the case of the Curie constant.[38] As our study shows the frequency dispersion in Curie constants as well as Curie temperatures, we can conclude that in our films, passive layer interference is due to both frequency and temperature dependences of the effective thickness of the passive layer. However, the frequency dispersion of those parameters seems to be very small (Fig. 5), reflecting a nominal effect of the film-interface passive layer for three of the films. Thus thickness dependence on the dielectric constant[31] is very small to count. Hence, according to Fig. 4(b), we can say that 1 mol % La doping increases the dielectric constant of PZ, while the next extent of doping starts to decrease in dielectric constant with respect to 1 mol % doping.

E. ac conductivity and Arrhenius plot

Temperature dependent ac conductivities of the thin films with different extents of La modification have been shown in Fig. 6. The ac conductivities of the films have been analyzed by the following relation:

$$\sigma_{ac} = 2\pi f \varepsilon_0 \varepsilon' \tan \delta, \tag{10}$$

where ε_0 is the permittivity of free space, f is the frequency, ε' is the relative dielectric constant, and $\tan \delta$ is the dissipation factor. For every film it has been seen that at low temperatures, in a log-log plot, ac conductivity exhibited the linear relationship with frequency at lower frequency region, whereas at higher frequency region, it has shown a strong frequency dependent behavior according to power law given below:

$$\sigma_{ac} = A\omega^n, \tag{11}$$

where $\omega = 2\pi f$ and n are functions of temperature and A is a constant. The n values for the films have been shown in Table I. In general, the n value lies between 0 and 1, and decreases with increasing temperature. Though the n value increases with decreasing temperature, in our cases it has exceeded the upper limit. Though within the 10^3 Hz frequency range the n value has been seen to be below unity, above that the value has increased in present study and it can be attributed as the ω^2 region. It is evident from the literatures that ω^2 dependence is the result of relatively small but finite resistances created by the thin film contacts.[39] According to Lakatos and Abkowitz,[39] three component equivalent network (Fig. 7) can be used to describe the experimental situation, where R_b and C_b are kept parallel as resistance and capacitance, respectively, to replicate the bulk sample and R_c is the resistance of the contacts in a series with a sample. According to this network, the parallel conductance and capacitance can be written as a function of frequency, given below:

$$G_p = \frac{1}{R_b} \left[\frac{(1 + R_c/R_b) + \omega^2 R_c R_b C_b^2}{(1 + R_c/R_b)^2 + \omega^2 R_c^2 C_b^2} \right], \tag{12}$$

$$C_p = C_b \left[\frac{1}{(1 + R_c/R_b)^2 + \omega^2 R_c^2 C_b^2} \right]. \tag{13}$$

For simplicity if we assume R_b is frequency independent, and if $R_c/R_b \ll 1$, $G_p \approx 1/R_b$ up to the frequency $\omega_1 = [(R_c R_b)^{1/2} C_b]^{-1}$. From these relations, it is clear that the larger the R_b is, the smaller the ω_1 becomes. Therefore the effect of contact resistance plays an important role for highly insulating materials. At frequency $\omega_2 = (R_c C_b)^{-1}$, G_p saturates at the value of $1/R_c$. Between ω_1 and ω_2, G_p is proportional to ω^2. If R_b is frequency dependent, Eqs. (12) and (13) are still useful, where the conditions are $R_b \propto \omega^{-n}$ and $n < 2$. The ac conductivity of our samples at low frequency region is almost frequency independent compared to high frequency, and that indicates that the frequency dependence of the bulk resistance is small. According to Maxwell[40] and Wagner,[41] any solid consisting of phases with different conductivities increase with frequency, because at high frequencies localized charge carrier motion makes it possible to take maxi-

[This article is copyrighted as indicated in the article. Reuse of AIP content is subject to the terms at: http://scitation.aip.org/termsconditions. Downloaded to] IP: 128.189.204.254 On: Thu, 11 Dec 2014 11:37:02

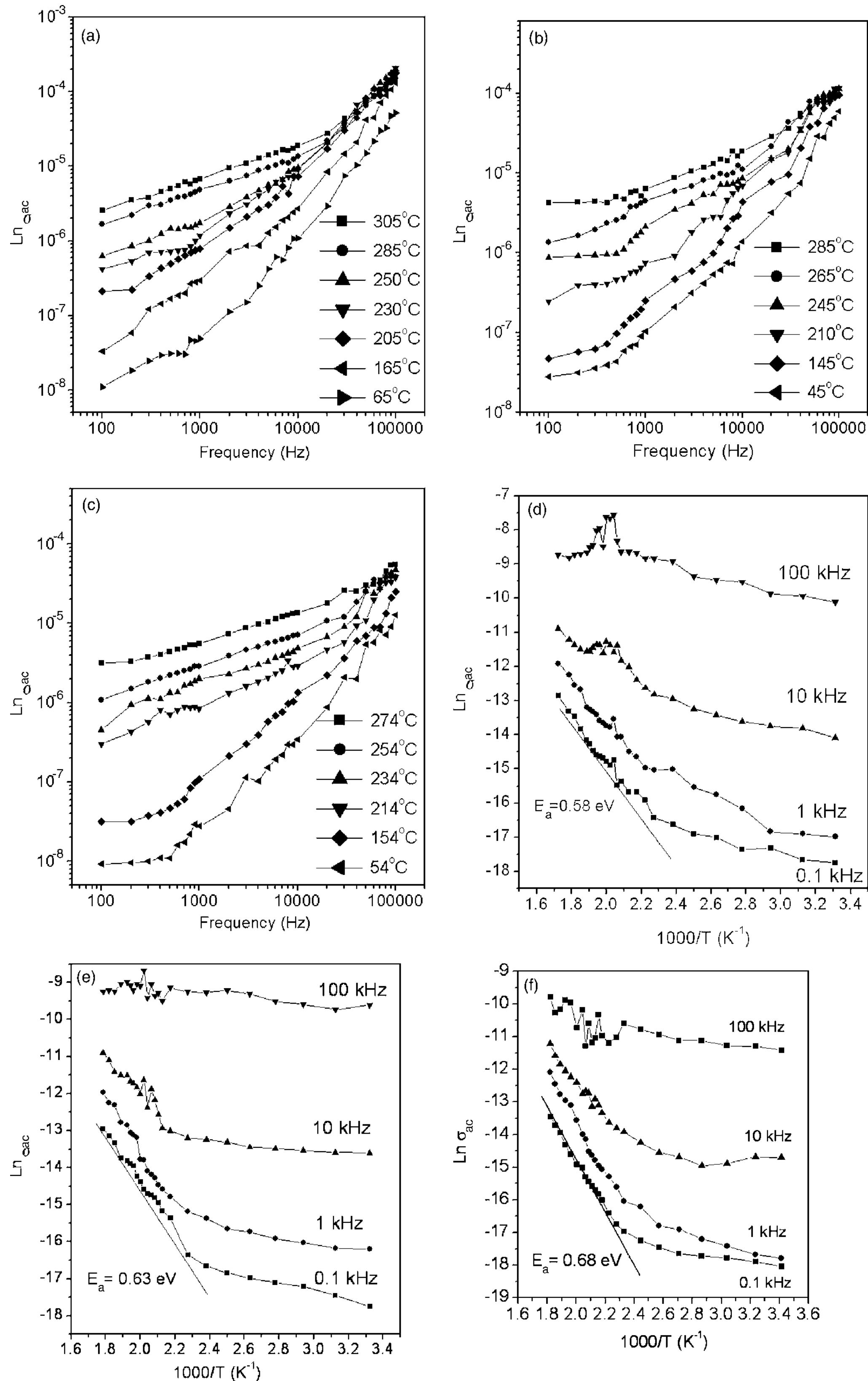

FIG. 6. ac conductivity as a function of frequency (a) for pure PZ, (b) for 1 mol % La-modified PZ, and (c) for 2 mol % La-modified PZ, where (d), (e), and (f) are Arrhenius plots of their ac conductivities respectively.

mum advantage of this well conducting regions, while at low frequencies charge transport must be extended over longer distances and is limited by bottlenecks of poorly conducting regions. But that phenomenon must obey the universal power law, Eq. (11), with the condition that $0<n<1$. A similar kind of activity was explained in detail by Jonscher where an equivalent circuit was taken as "resistance in series with parallel G-C combination"[42] (where G is conductance and C is

[This article is copyrighted as indicated in the article. Reuse of AIP content is subject to the terms at: http://scitation.aip.org/termsconditions. Downloaded to] IP: 128.189.204.254 On: Thu, 11 Dec 2014 11:37:02

TABLE I. *n* values, according to universal power law of ac conductivity, at different frequency regions and at different temperatures.

Films	Temperatures (in °C)	*n* values (within 10^2-10^3 Hz)	*n* values (within 10^3-10^5 Hz)
Pure PZ	65	0.54	1.76
	305	0.43	1.11
1 mol % La doped	65	0.45	1.74
	285	0.30	0.77
2 mol % La doped	54	0.51	1.59
	274	0.35	0.70

capacitance). Therefore in our case the conductivity at high frequency region is the manifestation of the electrode effect, whereas the passive layer effect in our films was already justified to be nominal.

In Fig. 6, the Arrhenius plot derived from the ac conductivity of the films shows two different regions corresponding to two different activation energies. For pure PZ it has been seen that at the temperature range of 305–165 °C the activation energy is 0.58 eV at 100 Hz, whereas in the case of 1 mol % La doped PZ has the activation energy of 0.63 eV in the temperature range of 285–165 °C at 100 Hz, and within the range of 274–164 °C, 2 mol % La doped PZ shows the activation energy of 0.68 eV at the same frequency. The activation energy for pure PZ is found to be in good agreement with the earlier reported values in Pb-based thin films, and this activation energy is attributed to the excitation energy of the trapped charge carriers[43] that are lying, in our case, in the band gap at a depth of 0.58 eV from the

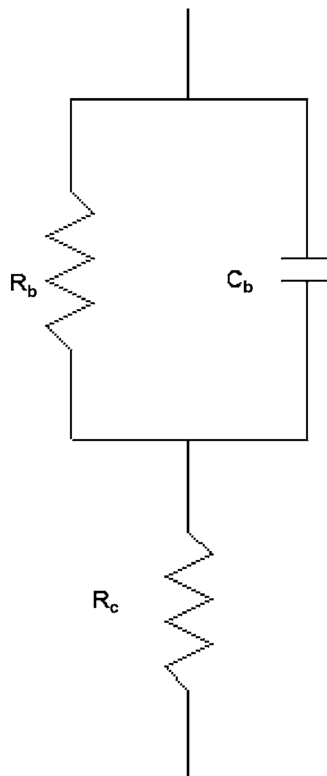

FIG. 7. Schematic representation of the electroded sample under dielectric measurement.

bottom of the conduction band. These sites are known as shallow trap states, and they are lying above the Fermi energy level.[43] So for all of the films ac conduction is supposed to be the cause of shallow trap controlled space charge current conduction in the bulk sample as the band gap energy in PZ ceramic is 3.93 eV.[44] The conduction electrons can be created from the donor states as a possible consequence of oxygen vacancies, as

$$O_O = \frac{1}{2}O_2 + V_{\ddot{O}} + 2e', \quad (14)$$

where O_O represents an oxygen ion situated at the oxygen site of a perovskite crystal and $V_{\ddot{O}}$ means an oxygen vacancy, which liberates two free electrons (denoted by e') very near to conduction band giving rise to a lower activation energy at low temperature region. In the case of high temperature region the high activation energy implies that there is a possibility that ionic charge carriers such as oxygen vacancies play a role in the conductivity.[45] Hence, among the two activation energy regions, one is supposed to be dominated by trapped electrons and another one by oxygen vacancies. According to Bharadwaja and co-workers,[19,46] the effect of donor La^{3+} doping in PZ- or Pb-based perovskite thin films can be considered to be between the following two extreme cases:

(i) with PbO loss, for which the defect equation reads

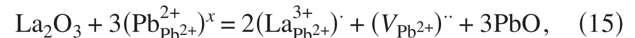

$$La_2O_3 + 3(Pb^{2+}_{Pb^{2+}})^x = 2(La^{3+}_{Pb^{2+}})^{\cdot} + (V_{Pb^{2+}})^{\cdot\cdot} + 3PbO, \quad (15)$$

in which two La ions would replace three Pb ions, creating a doubly negatively charged vacant Pb site so that Pb vacancies will dominate and try to capture a greater number of holes acting as deep traps, and

(ii) without PbO loss, for which the defect equation reads

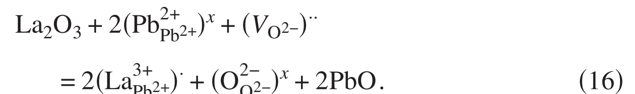

$$La_2O_3 + 2(Pb^{2+}_{Pb^{2+}})^x + (V_{O^{2-}})^{\cdot\cdot} = 2(La^{3+}_{Pb^{2+}})^{\cdot} + (O^{2-}_{O^{2-}})^x + 2PbO. \quad (16)$$

The above equation leads to the reduction of the oxygen vacancies with La occupation at Pb sites; i.e., two La ion occupancies compensate one oxygen vacancy. Thus decreasing *p*-type concentration, resistivity of the material can be improved. However, in most studies increase in resistivity of lead-based perovskite thin films was observed on La doping,[47,48] and in our cases, a decrease in the resistivity caused an electrode-dominated feature. So if we take the extreme phenomenon such as that without a PbO loss, it leads to films with oxygen vacancy compensation that reduces the shallow trap concentration and leads to an increase in the activation energies.[19] In our case, with the La doping the activation energy was seen to increase with increase in the La doping. The same phenomenon can be seen if we consider the PbO loss where Pb vacancies try to capture a greater number of holes acting as deep traps. The nonlinear shape of the Arrhenius plot implies a change in activation energy with temperature, which indicates that, at different temperatures, there are different mechanisms involved in the ac conduction mechanism. It has been observed that in the case of pure PZ film, before the horizontal region started,

[This article is copyrighted as indicated in the article. Reuse of AIP content is subject to the terms at: http://scitation.aip.org/termsconditions. Downloaded to] IP: 128.189.204.254 On: Thu, 11 Dec 2014 11:37:02

there was a kink in the conductivity followed by a decrease in conductivity even in higher temperature regions. This can be explained by the transition from one region of the sample to another.[49] The ac conductivity is seen to decrease with the increase of La doping, and the more the La doping is, the more the electrode effect prevails. At higher frequencies, temperature dependent phenomena have been seen to be obscured, and different mechanisms of the ac conductivity process have not been noticed. Though there are other mechanisms to describe the ω^2 dependence of the ac conductivity, they are more applicable for fast ion conductor.[50] Based on these arguments, the present observed conductivity behavior is claimed to be strongly coupled with electrode effect.

IV. CONCLUSIONS

In our present study, preparation of highly oriented (110) PZ and La-modified thin films using PVP has been reported. SEM micrographs have been shown for surface morphology and for the dense feature of the films with La doping. The field-forced AFE-FE phase transformations of preferred (110) oriented PZ and La-modified PZ thin films have been investigated, and the effect of electrostatic interaction between dopant and oxygen ions in PZ thin films has been observed. As it is well known that the dielectric property of a thin film is affected by its structural heterogeneity, the passive layer interference is typified by the Curie-Weiss law. The temperature dependencies of the dielectric properties of pure PZ and La-modified PZ thin films have been reported. The quality of the film was justified by minimum frequency dispersion in dielectric constants, Curie constants, and Curie temperatures. ac conductivity and the corresponding Arrhenius plot have been presented. The ω^2 dependence of the ac conductivity of the films is justified as the electrode effect.

[1]M. H. Francombe, Thin Solid Films **13**, 413 (1972).
[2]D. L. Polla and L. F. Francis, MRS Bull. **21**, 59 (1996).
[3]L. E. Cross and S. Trolier-McKinstry, Encyclopedia of Applied Physics, Vol. 21, (Wiley-VCH, New York, 1997), p. 429.
[4]S. Trolier-McKinstry, C. A. Randall, J. P. Maria, C. Theis, D. G. Schlom, J. Shephard, Jr., and K. Yamakawa, Mater. Res. Soc. Symp. Proc. **433**, 363 (1996).
[5]S. Trolier-McKinstry, P. Aungkavattana, F. Chu, J. Lacey, J. P. Maria, J. F. Shepard, T. Su, and F. Xu, Mater. Res. Soc. Symp. Proc. **493**, 59 (1998).
[6]K. Uchino, S. Nomura, L. E. Cross, S. J. Jang, and R. E. Newnham, J. Appl. Phys. **51**, 1142 (1980).
[7]W. Y. Pan, Q. M. Zhang, A. Bhalla, and L. E. Cross, J. Am. Ceram. Soc. **72**, 571 (1989).
[8]P. Yang and D. A. Pyne, J. Appl. Phys. **71**, 1361 (1992).
[9]B. Xu, Y. Ye, and L. E. Cross, J. Appl. Phys. **87**, 2507 (1999).
[10]G. Shirane, E. Sawaguchi, and Y. Takagi, Phys. Rev. **84**, 476 (1951).
[11]E. Sawaguchi, H. Maniwa, and S. Hoshino, Phys. Rev. **83**, 1078 (1951).
[12]F. Jona, G. Shirane, F. Mazzi, and R. Pepinsky, Phys. Rev. **105**, 849 (1957).
[13]G. Shirane and S. Hoshino, Acta Crystallogr. **7**, 203 (1954).
[14]K. D. Budd, S. K. Dey, and D. A. Pyne, Br. Ceram. Proc. **36**, 107 (1985).
[15]F. Wang, K. K. Li, and G. H. Haerteling, Opt. Lett. **17**, 1122 (1992).
[16]T. Tani, J.-F. Li, D. Viehland, and D. A. Payne, J. Appl. Phys. **75**, 3017 (1994).
[17]G. R. Bai, H. L. M. Chang, D. J. Lam, and Y. Gao, Appl. Phys. Lett. **62**, 1754 (1993).
[18]S. Chattopadhyay, P. Ayyub, V. R. Pakar, M. S. Muttani, S. P. Pai, S. C. Purandare, and R. Pinto, J. Appl. Phys. **83**, 7808 (1998).
[19]S. S. Bharadwaja and S. B. Krupanidhi, Thin Solid Films **423**, 88 (2003).
[20]X. Dai, J. Li, and D. Viehland, Phys. Rev. B **51**, 2651 (1995).
[21]S. Takenaka and H. Kozuka, Appl. Phys. Lett. **79**, 3485 (2001).
[22]S. Y. Chen and I. W. Chen, J. Am. Ceram. Soc. **77**, 2332 (1994).
[23]Z. Huang, Q. Zhang, and R. W. Whatmore, J. Mater. Sci. Lett. **17**, 1157 (1998).
[24]Z. Huang, Q. Zhang, and R. W. Whatmore, J. Appl. Phys. **85**, 7355 (1999).
[25]X. G. Tang, L. L. Jiang, and A. L. Ding, Microelectron. Eng. **65**, 387 (2003).
[26]Q. Zou, H. Ruda, B. G. Yacobi, and M. Farrell, Thin Solid Films **402**, 65 (2002).
[27]L. Shebanov, M. Kusnetsov, and A. Sternberg, J. Appl. Phys. **76**, 4301 (1994).
[28]R. D. Klissurska and N. Setter, J. Am. Ceram. Soc. **78**, 1513 (1995).
[29]S. H. Kim, D. J. Kim, J. G. Hong, S. K. Streiffer, and A. I. Kingon, J. Mater. Res. **14**, 1371 (1999).
[30]G. H. Haertling, Ferroelectrics **116**, 51 (1991).
[31]S. S. N. Bharadwaja and S. B. Krupanidhi, Mater. Sci. Eng., B **B78**, 75 (2000).
[32]C. Sudhama *et al.*, J. Vac. Sci. Technol. B **11**, 1302 (1993).
[33]M. Sayer, A. Mansingh, A. K. Arora, and A. Lo, Integr. Ferroelectr. **1**, 129 (1992).
[34]S. L. Miller, R. D. Nasby, J. R. Schwank, M. S. Rodgers, and P. V. Dressendorfer, J. Appl. Phys. **68**, 6463 (1990).
[35]S. R. P. Smith, J. Phys.: Condens. Matter **10**, 9141 (1998).
[36]A. K. Tagantsev, M. Landivar, E. Colla, and N. Setter, J. Appl. Phys. **78**, 2623 (1995).
[37]O. G. Vendik and S. Zubko, J. Appl. Phys. **82**, 4475 (1997).
[38]M. Tyunina and J. Levoska, Phys. Rev. B **63**, 224102 (2001).
[39]A. I. Lakatos and M. Abkowitz, Phys. Rev. B **3**, 1791 (1971).
[40]J. C. Maxwell, *A Treatise on Electricity and Magnetism*, 3rd ed. (Clarendon, Oxford, 1891), Vol. 1.
[41]K. W. Wagner, Ann. Phys. **40**, 817 (1913).
[42]A. K. Jonscher, *Dielectric Relaxation in Solids* (Chelsea Dielectric, London, 1983), pp. 72–74.
[43]S. S. N. Bharadwaja and S. B. Krupanidhi, Thin Solid Films **391**, 126 (2002).
[44]V. I. Zametin, Phys. Status Solidi B **124**, 625 (1984).
[45]S. Bhattacharyya, S. S. N. Bharadwaja, and S. B. Krupanidhi, J. Appl. Phys. **88**, 4294 (2000).
[46]S. S. N. Bharadwaja, P. Victor, P. Venkateswarulu, and S. B. Krupanidhi, Phys. Rev. B **65**, 174106 (2002).
[47]E. M. Griswold, M. Sayer, D. T. Amm, and I. D. Calder, Can. J. Phys. **69**, 260 (1991).
[48]D. Dimos, R. W. Schwartz, and S. J. Lockwod, J. Am. Ceram. Soc. **76**, 5394 (1994).
[49]S. Bhattacharyya, Ph.D. thesis, Indian Institute of Science, 2001.
[50]C. Cramer and M. Buscher, Solid State Ionics **105**, 109 (1998).
[51]JCPDS Card No. 3-655, Megaw. H., Philips Lamps Ltd., Mitcham, Surrey, private communication.

[This article is copyrighted as indicated in the article. Reuse of AIP content is subject to the terms at: http://scitation.aip.org/termsconditions. Downloaded to] IP: 128.189.204.254 On: Thu, 11 Dec 2014 11:37:02